Tue-Af-Po2.06-11 [75] Analysis and application of discrete Halbach magnet array with unequal arc lengths and unequally-changed magnetization directions.

Author: Hailin Huang, Dawei Li, Ronghai Qu, Libing Jing
Huazhong University of Science and Technology, Wuhan, 430074, China

Introduction

Halbach PM array offers many attractive features: sinusoidal flux distribution, self-shielding effect, high fundamental field, low cogging torque, etc. Normal discrete Halbach array pursues a better flux distribution by increasing the number of segments per pole. However, a higher number of discrete segments also increase the cost of fabrication. Hence, optimization on other parameters is required to reach the optimal compromise between the cost and performance.

In this paper, a **general process** is presented to design an arbitrary Halbach PM array with multi-parameters: arc length of PM and gap, magnetization direction of PM segment. This process includes a universal **analytical model** and a **multi-objective optimizer**. In addition to the conventional type, a **new arrangement** of Halbach array with gap-symmetry-axis is also analyzed and validated by FEA. The effectiveness of a multi-objective optimization algorithm is examined. Owing to the clearness and flexibility of proposed model, more design requirements can be achieved.

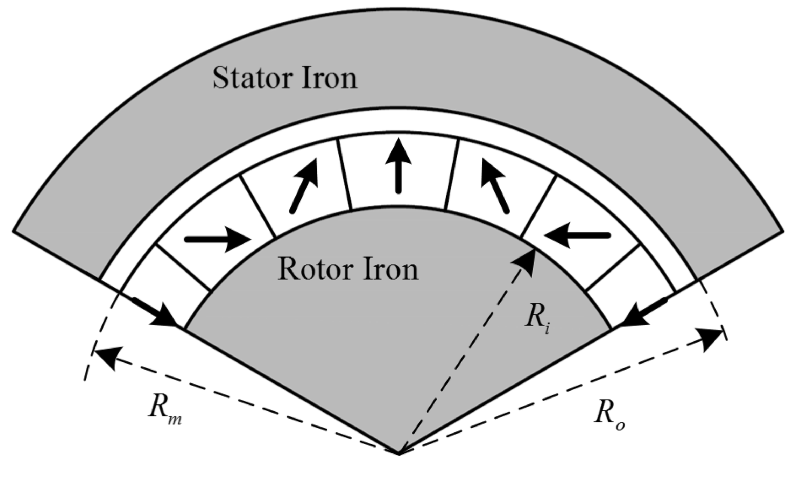

Fig. 1 Structure of 3-segment Halbach array in one pole-pair

General Analytical Models

A. PM-symmetry-axis Model | B. Gap-symmetry-axis Model

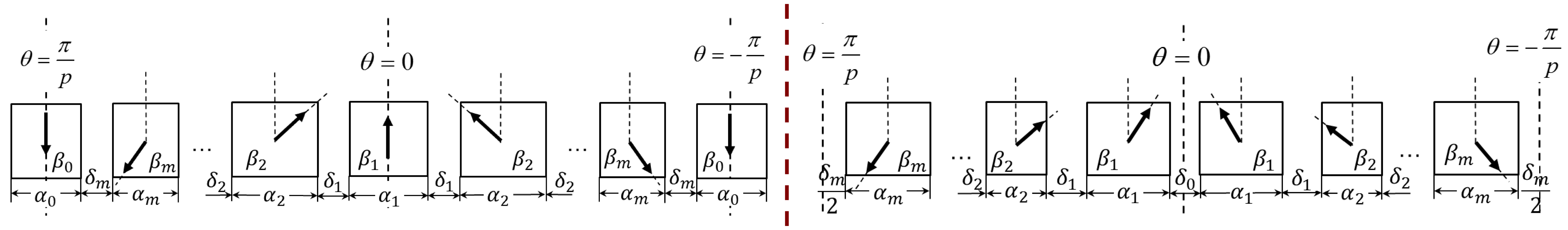

Relations Between Parameters

$\beta_1=0$, $\beta_0=\pi$

$$\frac{\pi}{p}=\frac{\alpha_0+\alpha_1}{2}+\sum_{i=1}^{m}(\delta_i+\alpha_i) \qquad \gamma_i=\sum_{k=1}^{i}(\delta_k+\alpha_k)-\delta_i-\frac{\alpha_1+\alpha_i}{2}$$

γ defines the angular position of each PM segment's center.

$$\frac{\pi}{p}=\frac{\delta_0+\delta_m}{2}+\sum_{i=1}^{m-1}\delta_i+\sum_{i=1}^{m}\alpha_i \qquad \gamma_i=\frac{\delta_0}{2}+\sum_{k=1}^{i-1}\delta_k+\sum_{k=1}^{i}\alpha_k-\frac{\alpha_i}{2}$$

Decomposition of Residual Magnetisation Vector $\boldsymbol{M}$

$$\boldsymbol{M}=M_r\vec{r}+M_\theta\vec{\theta}=\sum M_{rn}\cos(np\theta)+\sum M_{\theta n}\sin(np\theta)$$

According to the symmetry

A. PM-symmetry-axis Model:

$$M_r(\theta)=\begin{cases} M\cos(-\theta) & 0\le\theta\le\alpha_1/2 \\ M\cos(\beta_2-\theta+\gamma_2) & \gamma_2-\alpha_2/2\le\theta\le\gamma_2+\alpha_2/2 \\ \cdots & \\ M\cos(\beta_m-\theta+\gamma_m) & \gamma_m-\alpha_m/2\le\theta\le\gamma_m+\alpha_m/2 \\ -M\cos(-\theta+\pi/p) & \pi/p-\alpha_0/2\le\theta\le\pi/p \\ 0 & \text{others}\end{cases}$$

$$M_\theta(\theta)=\begin{cases} M\sin(-\theta) & 0\le\theta\le\alpha_1/2 \\ M\sin(\beta_2-\theta+\gamma_2) & \gamma_2-\alpha_2/2\le\theta\le\gamma_2+\alpha_2/2 \\ \cdots & \\ M\sin(\beta_m-\theta+\gamma_m) & \gamma_m-\alpha_m/2\le\theta\le\gamma_m+\alpha_m/2 \\ -M\sin(-\theta+\pi/p) & \pi/p-\alpha_0/2\le\theta\le\pi/p \\ 0 & \text{others}\end{cases}$$

B. Gap-symmetry-axis Model:

$$M_r(\theta)=\begin{cases} M\cos(\beta_1-\theta+\gamma_1) & \gamma_1-\alpha_1/2\le\theta\le\gamma_1+\alpha_1/2 \\ M\cos(\beta_2-\theta+\gamma_2) & \gamma_2-\alpha_2/2\le\theta\le\gamma_2+\alpha_2/2 \\ \cdots & \\ M\cos(\beta_m-\theta+\gamma_m) & \gamma_m-\alpha_m/2\le\theta\le\gamma_m+\alpha_m/2 \\ 0 & \text{others}\end{cases}$$

$$M_\theta(\theta)=\begin{cases} M\sin(\beta_1-\theta+\gamma_1) & \gamma_1-\alpha_1/2\le\theta\le\gamma_1+\alpha_1/2 \\ M\sin(\beta_2-\theta+\gamma_2) & \gamma_2-\alpha_2/2\le\theta\le\gamma_2+\alpha_2/2 \\ \cdots & \\ M\sin(\beta_m-\theta+\gamma_m) & \gamma_m-\alpha_m/2\le\theta\le\gamma_m+\alpha_m/2 \\ 0 & \text{others}\end{cases}$$

Fourier Expension of M_r and M_θ

'+' is for M_{rn}, and '−' is for $M_{\theta n}$

$$M_{rn},M_{\theta n}=\frac{2pM}{\pi}\cdot\sum_{i=1}^{m}\left[\frac{\sin(0.5(np+1)\alpha_i)\cos(np\gamma_i-\beta_i)}{np+1}\pm\frac{\sin(0.5(np-1)\alpha_i)\cos(np\gamma_i+\beta_i)}{np-1}\right]$$

$$M_{rn}=\frac{2pM}{\pi}\left\{\frac{1}{2}\left[\frac{\sin(0.5(np+1)\alpha_1)}{np+1}+\frac{\sin(0.5(np-1)\alpha_1)}{np-1}\right]+\sum_{i=2}^{m}\left[\frac{\sin(0.5(np+1)\alpha_i)\cos(np\gamma_i-\beta_i)}{np+1}+\frac{\sin(0.5(np-1)\alpha_i)\cos(np\gamma_i+\beta_i)}{np-1}\right]-\frac{np\cos(0.5\alpha_0)\sin(0.5np\alpha_0-n\pi)-\sin(0.5\alpha_0)\cos(0.5np\alpha_0-n\pi)}{(np+1)(np-1)}\right\}$$

$$M_{\theta n}=\frac{2pM}{\pi}\left\{\frac{1}{2}\left[\frac{\sin(0.5(np+1)\alpha_1)}{np+1}-\frac{\sin(0.5(np-1)\alpha_1)}{np-1}\right]+\sum_{i=2}^{m}\left[\frac{\sin(0.5(np+1)\alpha_i)\cos(np\gamma_i-\beta_i)}{np+1}-\frac{\sin(0.5(np-1)\alpha_i)\cos(np\gamma_i+\beta_i)}{np-1}\right]-\frac{np\sin(0.5\alpha_0)\cos(0.5np\alpha_0-n\pi)-\cos(0.5\alpha_0)\sin(0.5np\alpha_0-n\pi)}{(np+1)(np-1)}\right\}$$

Process from Residual Magnetization $\boldsymbol{M}$ to Flux Density $\boldsymbol{B}$

$$M_n=M_{rn}+npM_{\theta n} \qquad B_r=\sum B_{rn}\cos(np\theta) \qquad B_\theta=\sum B_{\theta n}\sin(np\theta)$$

- **Assumptions:** 1. Back iron has infinite permeance 2. End-effect and slot-effect are neglected.
- Through solving the governing Laplacian/quasi-Poissonian field equations in the air gap and magnet regions, analytical model of magnetic field distribution can be derived as shown.
- Two plus-minus signs differ the equation of B_{rn} and $B_{\theta n}$, '+' is for B_{rn}, and '−' is for $B_{\theta n}$.
- The derivation from slotless to slotted model of surface PM machine has already well solved by comformal mapping method or by subdomain model, which can also be applied in Halbach PM array. Moreover, the cogging torque, electromagnetic torque, back-EMF in Halbach PM machine can also be predicted through these methods.

$$B_{rn},B_{\theta n}=\pm\frac{\mu_0}{\mu_r}M_n\frac{np}{(np)^2-1}\left[\left(\frac{R_m}{r}\right)^{np+1}\pm\left(\frac{r}{R_o}\right)^{np-1}\left(\frac{R_m}{R_o}\right)^{np+1}\right]\times\frac{\left\{\left[\left(np-\frac{1}{np}\right)\frac{M_{rn}}{M_n}+\frac{1}{np}+1\right]\left[1-\left(\frac{R_i}{R_m}\right)^{2np}\right]+2\left(\frac{R_i}{R_m}\right)^{np+1}-2\right\}}{\frac{\mu_r+1}{\mu_r}\left[1-\left(\frac{R_i}{R_o}\right)^{2np}\right]-\frac{\mu_r-1}{\mu_r}\left[\left(\frac{R_m}{R_o}\right)^{2np}-\left(\frac{R_i}{R_m}\right)^{2np}\right]}$$

Validation by FEA

- Analytical models for both types are well validated by 2-D FEA when segment number of each pole m =2, 3, 4. Parameters of models are shown in Table I.
- When m increases, Radial flux distribution becomes more sinusoidal, and the peak of Tangential flux distribution becomes smaller, which represents a better performance.
- Despite the differences on flux distribution, two type of m-segment Halbach array have the same primary flux density and total harmonic distortion. It proves that Gap-symmetry-axis Model is as practical as the conventional one.

TABLE I
PARAMETERS OF THE FEA VERIFICATION MODEL

Parameter	Symbol	Value	Unit
Pole-pair number	p	3	-
Stator inner radius	R_o	51	mm
PM outer radius	R_m	50	mm
PM inner radius	R_i	40	mm
Thickness of PM	D_p	10	mm
Remanence of PM	B_r	1.25	T
Arc of gaps	δ_i	0	degree
Arc of PM segments	α_i	60/m	degree

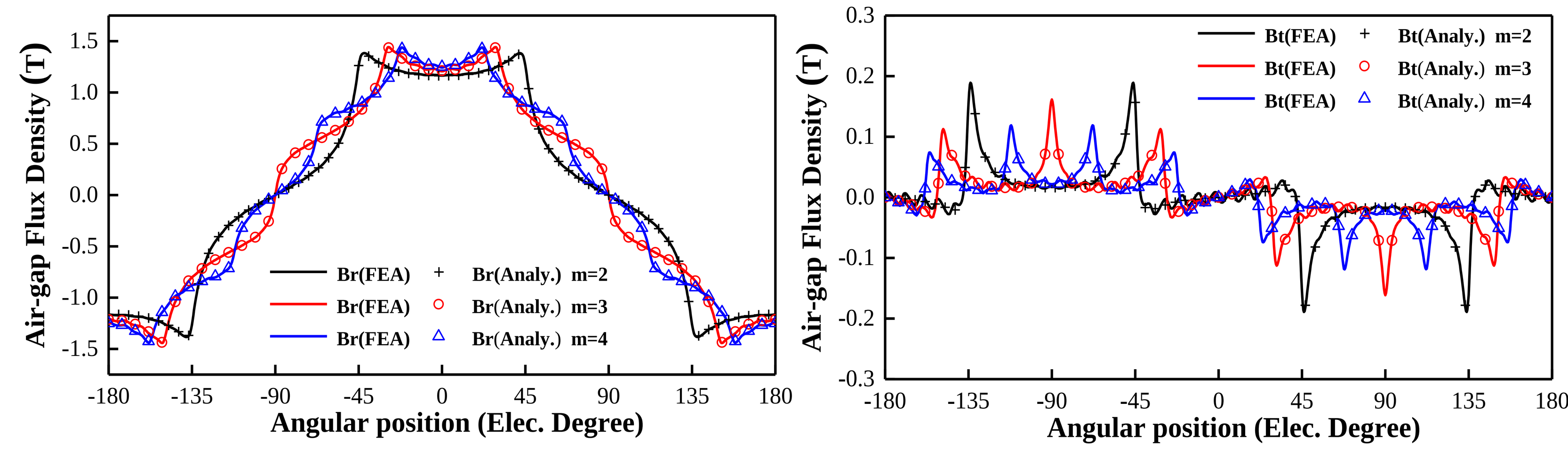

Fig. 3 **PM-symmetry-axis Halbach array.** Comparison of FEA and analytical predicted air-gap flux distribution when m=2, 3, 4. (a) Radial Br. (b) Tangential Bt.

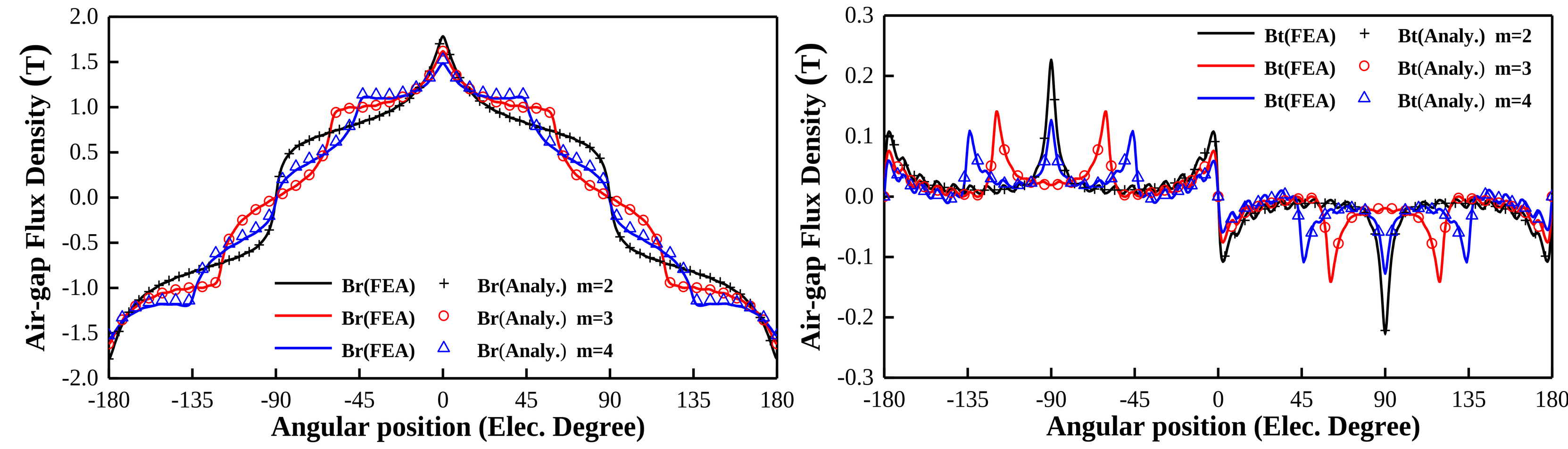

Fig. 4 **Gap-symmetry-axis Halbach array.** Comparison of FEA and analytical predicted air-gap flux distribution in Halbach array when m=2, 3, 4. (a) Radial Br. (b) Tangential Bt.

Multi-Objective Optimization

- An optimization on 3-segment Halbach array general model was given to examine the effectiveness.
- Created spots of 5 generations during the genetic optimized algorithm were differed by colors, which are gradually **getting closer to** Pareto front.
- The yellow Star in Fig. 5 locates the performance of the original type with equal arc and magnetization.
- Pareto front revealed by red line offers researchers valuable tradeoff information between objectives.
- Compared to the original one, optimized model has **better performances** on Br and THD, see Table II.
- Proposed process is more effective towards **different requirements**. For example, more than one main flux harmonics can be easily achieved by changing objectives of optimization, see Fig. 6, densities of 1st and 4th harmonics are both **greater than 0.8 T.**

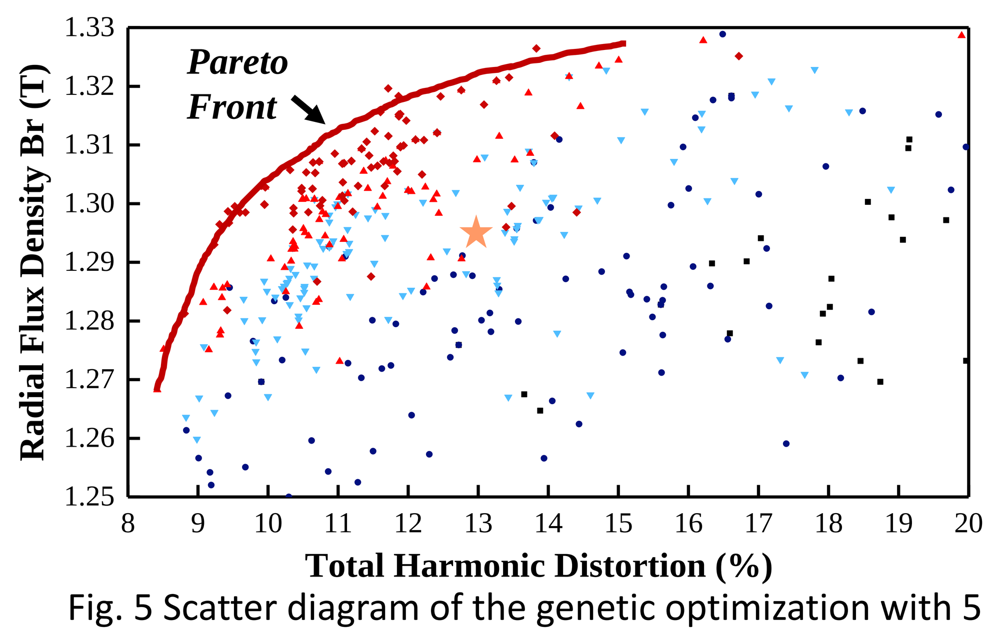

Fig. 5 Scatter diagram of the genetic optimization with 5 generations for 3-segment Halbach array.

TABLE II
COMPARISON OF ORIGINAL AND OTIMIZED HALBACH MODEL

Parameter	Orginal	Optimized	Effect
Primary flux density Br	1.295 T	1.310 T	+1.2%
Total harmonic distortion	12.9 %	10.2 %	-21%

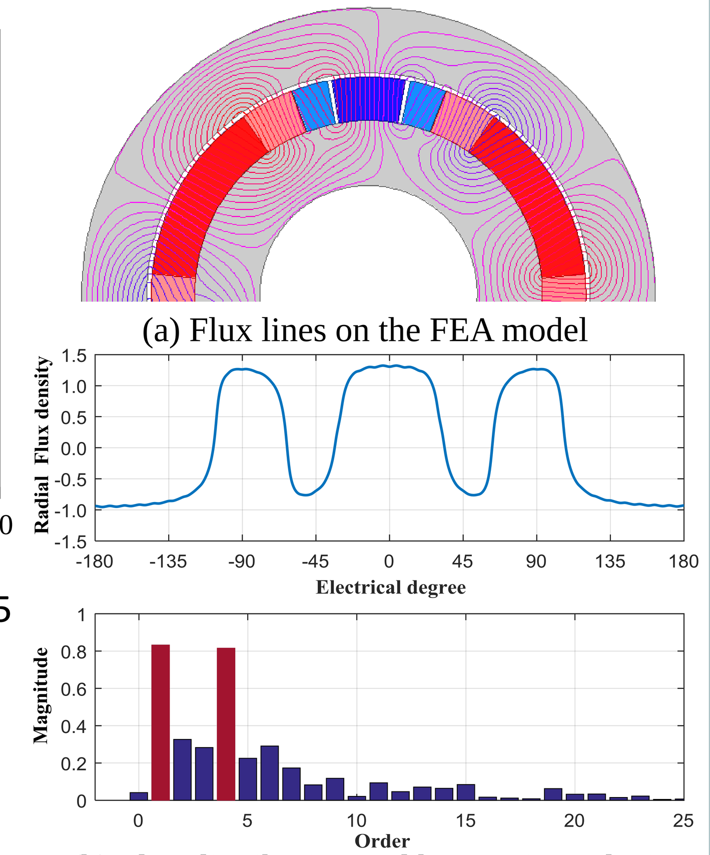

(b) Flux distribution and harmonic analysis
Fig. 6 Optimal model with 1st and 4th as main flux harmonics.

Conclusions

- **A general design process** of arbitrary Halbach arrays with accurate analytical models and a multi-objective optimizer has bee proposed.
- Both traditional and **a new type of arrangement** of Halbach array was calculated and validated by FEA, which are proved to be same effective.
- Through combining accurate analytical model with mathematical software, a simple and time-saving design optimization towards more cost efficiency and more extensive use for Halbach array can be achieved.
- The test on 3-segment PM array shows that after parameter design by optimizer, both fundamental flux density and THD of "unequal" Halbach array can be better than "equal" one. It proves the **necessity of parameter design** on Halbach PM array.
- **Special requirements** can be easily achieved via this process, Halbach array model with two main flux harmonics are given as an example.
- In the next researches, **more design and performance parameters** will be included into this process through existing methods for surface PM machines: stator slots, materials, modulating pieces, cogging torque, back-EMF, EM torque, etc.

Presented at the MT25 Conference, 2017 Aug. 27 – Sept. 1, Netherland, Amsterdam; Session: Tue-Af-Po2.06 [75]; ID Number: 1138 Poster: Mr. Hailin Huang.